HHS Public Access

Author manuscript

Nat Cell Biol. Author manuscript; available in PMC 2015 November 01.

Published in final edited form as:

Nat Cell Biol. 2015 May ; 17(5): 580–591. doi:10.1038/ncb3161.

HUMAN DEFINITIVE HAEMOGENIC ENDOTHELIUM AND ARTERIAL VASCULAR ENDOTHELIUM REPRESENT DISTINCT LINEAGES

Andrea Ditadi[1], **Christopher M. Sturgeon**[1,2], **Joanna Tober**[3], **Geneve Awong**[1], **Marion Kennedy**[1], **Amanda Phillips**[3], **Lisa Azzola**[4], **Elizabeth S. Ng**[4,5], **Edouard Stanley**[4,5,6], **Deborah L. French**[7], **Xin Cheng**[7,8], **Paul Gadue**[7], **Nancy Speck**[3], **Andrew G. Elefanty**[4,5,6], and **Gordon Keller**[1,*]

[1]McEwen Centre for Regenerative Medicine, University Health Network, Toronto ON Canada

[3]Cell and Developmental Biology, University of Pennsylvania, Philadelphia PA, United States

[4]Murdoch Children's Research Institute, The Royal Children's Hospital, Parkville VIC, Australia

[5]Department of Anatomy and Developmental Biology, Faculty of Medicine, Nursing and Health Sciences, Monash University Clayton VIC, Australia

[6]Department of Paediatrics, Faculty of Medicine, Dentistry and Health Sciences, University of Melbourne, Parkville VIC, Australia

[7]Department of Pathology and Laboratory Medicine, Children's Hospital of Philadelphia, Philadelphia PA, United States

Abstract

The generation of haematopoietic stem cells (HSCs) from human pluripotent stem cells (hPSCs) will depend on the accurate recapitulation of embryonic haematopoiesis. In the early embryo, HSCs develop from the haemogenic endothelium (HE) and are specified in a Notch-dependent manner through a process named endothelial-to-haematopoietic transition (EHT). As HE is associated with arteries, it is assumed that it represents a subpopulation of arterial vascular endothelium (VE). Here we demonstrate at a clonal level that hPSC-derived HE and VE represent separate lineages. HE is restricted to the $CD34^{+}CD73^{-}CD184^{-}$ fraction of day 8 embryoid bodies (EBs) and it undergoes a NOTCH-dependent EHT to generate $RUNX1C^{+}$ cells with multilineage potential. Arterial and venous VE progenitors, by contrast, segregate to the $CD34^{+}CD73^{med}CD184^{+}$ and $CD34^{+}CD73^{hi}CD184^{-}$ fractions, respectively. Together, these findings identify HE as distinct from VE and provide a platform for defining the signalling pathways that regulate their specification to functional HSCs.

* to whom correspondence should be addressed: gkeller@uhnresearch.ca.

[2]Present address: Department of Internal Medicine, Hematology Division, Washington University School of Medicine, St. Louis MO, United States

[8]Present address: Institute of Biochemistry and Cell Biology, Shanghai Institutes for Biological Sciences, Chinese Academy of Sciences, Shanghai, China.

Keywords

embryonic stem cell; pluripotent; definitive haematopoiesis; haemogenic endothelium; RUNX1C; vascular endothelium; arterial; venous; CD184; CD73; DLL4; Notch signalling; multipotent progenitor

Introduction

Human pluripotent stem cells (hPSCs) represent an unlimited source of therapeutically important haematopoietic cells, including transplantable haematopoietic stem cell (HSCs) for the treatment of haematological disorders. However, despite significant advances in our ability to differentiate hPSCs to diverse haematopoietic cell types[1-4], the generation of HSCs *in vitro* has been challenging. This difficulty in deriving HSCs is due in part to the complex structure of the embryonic haematopoietic system that consists of separate programs that display different potential and are specified at distinct times during development[5]. HSCs are generated from the definitive haematopoietic program that is initiated in different sites within the embryo following the onset of primitive haematopoiesis that develops at an earlier stage and generates a restricted subset of lineages[8].

Studies from different model organisms have shown that HSCs develop from a progenitor population known as haemogenic endothelium (HE) that expresses endothelial markers and is thought to derive directly from the developing arterial vasculature[6-9]. Kinetic analyses of the haemogenic sites in the early embryo combined with time-lapse studies *ex vivo* have shown that during specification of the haematopoietic fate, HE undergoes an endothelial-to-haematopoietic transition (EHT) to generate blood cell progenitors[6-8] that subsequently mature to give rise to functional HSCs[9].

The identification of hPSC-derived HE has been challenging due to the fact that the primitive program also transitions through a HE population that is indistinguishable from definitive HE based on expression of cell surface markers[10]. Given these similarities, it is essential to be able to distinguish the two programs in order to monitor the development of definitive HE. We have recently shown that primitive and definitive haematopoiesis differ in their requirement for activin/nodal/TGFβ and Wnt/β-catenin signalling at the mesoderm specification stage and that through appropriate manipulation, it is possible to deplete the hPSC-derived populations of the primitive haematopoietic lineages[2, 10]. Dependency on Notch signalling is also a distinguishing feature of these programs, as loss-of function studies in vertebrate embryos have demonstrated that this pathway is essential for specification of HSCs and definitive progenitors, but dispensable for primitive haematopoiesis[11-14].

Here, we have exploited these differences to isolate and characterize hPSC-derived definitive HE. We show that this HE can be distinguished from VE based on cell surface marker expression and that it can progress through the EHT in a NOTCH-dependent fashion to to generate myeloid, erythroid and lymphoid progeny. Together, these findings provide strong evidence that the hPSC-derived definitive HE represents the *in vitro* equivalent of the HE in the early embryo that gives rise to the HSC.

Results

hPSC-derived HE undergoes EHT to generate haematopoietic progeny

We previously identified a definitive $CD34^+CD43^-$ population that expresses HE markers ($CD31^+CD144^+KDR^+cKIT^{lo}$) and displayed the capacity to generate T lymphoid, erythroid and myeloid cells following culture on stromal cells[2, 10]. To be able to monitor the EHT of this population, we isolated hESC-derived $CD34^+$ cells and cultured them on Matrigel, in the presence of haematopoietic cytokines known to promote and sustain haematopoietic differentiation[15-17] (EHT culture, Fig. 1a). Under these conditions, the cells rapidly formed an adhesive monolayer that underwent the EHT as demonstrated by the emergence of round cells within 3 to 4 days of culture and of a population of $CD45^+$ cells by day 7 (Fig. 1b-c). Examination of the EHT cultures with time-lapse imaging revealed that the adherent cells gradually acquire CD45 expression and then give rise to non-adherent $CD45^+$ haematopoietic cells (Supplementary Movie 1). Immunostaining analyses showed that the emerging round cells co-express endothelial (CD144) and haematopoietic (CD45) surface markers as well as cKIT, a marker indicative of EHT[7, 18] (Fig. 1d, Supplementary Movie 2).

To monitor definitive haematopoiesis in the day 8+7 population, we isolated the different CD34/CD45 fractions and assayed them for their hematopoietic potential and for expression of key genes associated with embryonic haematopoiesis including *MYB*,*RUNX1C*, *TAL1* and *GATA2* (Fig. 1e-h). T lymphoid progenitors were only detected in the two $CD34^{+(med/lo)}$ $CD45^+$ fractions, whereas myelo/erythroid progenitors were found in all 3 $CD45^+$ fractions (Fig. 1f-g). RT-PCR analyses showed that expression of *MYB*, *RUNX1C*, *TAL1* and *GATA2* was significantly higher in the 3 $CD45^+$ haematopoietic fractions than in the $CD34^{hi}CD45^-$ fraction and the input day 8 $CD34^+$ population (Fig. 1h). The $CD34^{hi}CD45^-$ -derived fraction showed no haematopoietic potential, suggesting that it consists of only endothelial progenitors. The erythroid colonies generated from $CD34^{med}CD45^+$-derived progenitors at the end of EHT culture expressed levels of foetal globin *HBG* similar to that found in total mononuclear foetal liver cells and significantly higher than the levels in hESC-derived primitive erythroid colonies (Ery^P) (Supplementary Fig. 1). As previously reported [2, 10], these HE-derived colonies retain expression of the embryonic globin *HBE* and show very low levels of the adult globin *HBB* a pattern similar to that observed in human foetal liver-derived eythroid colonies[22]. Collectively, these findings suggest that the erythroid colonies generated from the HE represent the onset of definitive haematopoiesis.

T cell progenitors generated following the EHT express RUNX1C

To provide better resolution of the emerging definitive HE and its EHT, we next differentiated a reporter human embryonic stem cell (hESC) line in which EGFP expression is driven by the *RUNX1C* promoter (*R1C*-GFP, described in Supplementary Fig. 2a-i). In the mouse embryo, the *Runx1c* isoform is first expressed in the earliest definitive haematopoietic progenitors[19]. *RUNX1C*-EGFP expression was not detected in the day 8 HE $CD34^+$ population nor in $CD34^+$ populations identified at earlier stages of development (Supplementary Fig. 3a). Following EHT culture, the *R1C*-GFP-derived $CD34^+$ cells generated the same spectrum of $CD34^+CD45^+$ fractions observed in the H1-derived population (Fig. 2a upper panel). A distinct *RUNX1C*-$EGFP^+CD34^{med}$ fraction was also

detected at this time (Fig. 2a lower panel). Kinetic analyses showed that *RUNX1C*-EGFP^{+}CD34^{med} cells emerged as early as day 4 of EHT culture and by day 8+5, approximately half of the fraction also co-expressed CD144 and CD45 (Fig. 2b), a pattern found on HSCs in the E11.5 mouse AGM are CD144^{+}CD45^{+}.

Analyses of the different fractions in the day 8+5 population showed that only the *RUNX1C*-EGFP^{+}CD34^{med} cells gave rise to T lymphocytes (Fig. 2c,d). These cells also expressed the highest levels of *MYB, RUNX1C, TAL1* and *GATA2* (Fig. 2e). Together, these findings demonstrate that the hESC-derived CD34^{+} population contains HE that undergoes EHT to generate a CD34^{med}CD45^{+}*RUNX1C*$^{+}$ population that displays definitive haematopoietic potential.

To determine if RUNX1C shows the same definitive restricted expression pattern in the hESC-derived cultures as it does in the mouse embryo[19], we next analysed *R1C*-GFP-derived primitive haematopoietic populations. As a first approach we isolated the KDR^{+}CD235a^{+} and KDR^{+}CD235a^{-} fractions from day 3 Activin A-induced EBs as we have recently shown that they represent progenitors of the primitive and definitive haematopoietic programs, respectively[10]. The sorted cells were aggregated and cultured for 6 days to generate either primitive or definitive CD34^{+}CD43^{-} HE, as described in our previous study[10]. These respective HE populations were isolated and assayed in our EHT culture conditions. Although both HE populations generated CD45^{+} cells, only the definitive KDR^{+}CD235^{-} progenitors gave rise to *RUNX1C*-EGFP^{+} cells (Fig. 2f). With the second approach, we analysed different staged EBs generated in the presence of the WNT inhibitor IWP2 as we have shown this manipulation promotes primitive haematopoiesis at the expense of the definitive haematopoietic program[10]. *RUNX1C*-EGFP expression was not detected in the EB cells at any stage, or in the EHT cultures generated from the day 8 CD34^{+}CD43^{-} progenitors (day 8+7) (Supplementary Fig. 3b). Taken together, these findings provide strong evidence that *RUNX1C*-EGFP expression is restricted to the definitive haematopoietic program in the hPSC differentiation cultures.

NOTCH signalling is essential for the EHT

If the emergence of the CD34^{+}CD45^{+}*RUNX1C*$^{+}$ population is reflective of the onset of human definitive haematopoiesis its development should, at some stage, be dependent on NOTCH signaling. To investigate this, we treated CHIR-induced hPSC-derived cells at 2 different time intervals (day 3–8 EBs or day 8–8+7 EHT culture) with the chemical NOTCH inhibitor, γ-secretase inhibitor L-685,458 (GSI). Inhibition of NOTCH between days 3 and 8 of differentiation during the haematopoietic and vascular lineages specification stage (Fig. 1a) reduced NOTCH target gene expression (*HES1*, *HEY1* and *HES5*; Supplementary Fig. 4a) and led to a 2-fold increase in the proportion of CD34^{+} cells detected at day 8 (Fig. 3a). Blocking the pathway at this stage did not dramatically affect the emergence of the definitive haematopoietic program, as the treated CD34^{+} population underwent EHT and contained T cell progenitors (Fig. 3b-c)

In contrast, treatment of the isolated CD34^{+} cells with GSI during the EHT culture prevented the formation of the non adhesive round cells, reduced the size of the CD45 population that developed in the H1-derived cultures, and blocked the emergence of

RUNX1C-EGFP$^+$ cells in the *R1C*-GFP-derived cultures (Fig. 3d-f). Consistent with these observations, GSI-treatment at this stage also inhibited the development of myelo/erythroid and T cell progenitors (Fig. 3g-i). These findings indicate that the haematopoietic specification of HE during the EHT is NOTCH-dependent.

To define more precisely the NOTCH-dependent stage, we next added GSI for defined intervals during the EHT culture. As shown in Fig. 3l and Supplementary Fig. 4b, the largest reduction in the size of the CD45$^+$ population was observed when GSI was included for the first 3 days of culture, the stage coinciding with onset of EHT (Fig. 1c). Collectively, these findings demonstrate that haematopoietic specification of the CD34$^+$ HE population is dependent on NOTCH signalling, indicating that the emerging blood cell lineages represent the definitive program. Additionally, they show that the NOTCH pathway is essential for the EHT stage of development, but not for the specification of the CD34$^+$ HE.

Enrichment of HE in the CD34$^+$ population

To enrich for HE within the CD34$^+$ population, we next analysed it for expression of CD73 as recent studies showed that this marker distinguishes haemogenic and non-haemogenic progenitors at early stages in hPSC differentiation cultures[20-22]. We also monitored CD184 expression, which demarcates arterial endothelium in the mouse embryo and in mESC-derived endothelial populations[23, 24]. The expression of these 2 markers resolved the following 3 fractions in the day 8 CD34$^+$ population: CD73$^-$CD184$^-$, CD73^{med}CD184$^+$ and CD73^{hi}CD184$^-$ (Fig. 4a). When cultured under EHT conditions, all 3 populations generated an adhesive monolayer consisting of cells with endothelial morphology. However, only the CD73$^-$CD184$^-$-derived population underwent EHT and gave rise to CD45$^+$ cells (Fig. 4b), CD34$^+$*RUNX1C*$^+$cells (Fig. 4c) and myeloid/erythroid (Fig. 4d) and T cell progenitors (Fig. 4e). Limiting-dilution analyses revealed a frequency of 1/35 T cell progenitors in the CD73$^-$CD184$^-$ population compared to 1/700 in the nonfractionated CD34$^+$ population, indicating a significant enrichment in HE. As observed with the unfractionated CD34$^+$ population, the transition of the CD73$^-$CD184$^-$ cells to a haematopoietic fate appears to be a NOTCH dependent event, as addition of GSI during the EHT culture strongly reduced the development of the myeloid and erythroid progenitors (Fig. 4d).

Kinetic analyses revealed that a small CD34$^+$CD184$^+$ population was detectable as early as day 4 of differentiation (Supplementary Fig 5a, left panels). All 3 fractions were present by day 6 (Supplementary Fig 5a, right panels), the earliest stage at which we were previously able to measure T cell progenitors[2]. As observed with the day 8 population, the EHT potential as well as lymphoid and erythroid/myeloid progenitors were only detected in the CD73$^-$CD184$^-$ fraction at day 6 (Supplementary Fig 5b-d**)**. Generation of the erythroid/myeloid progenitors from the day 6 HE was also dependent on NOTCH signalling as their development was inhibited by the addition of GSI during the EHT culture (Supplementary Fig 5d).

The day 8 CD34$^+$ population isolated from EBs generated from the *R1C*-GFP cell line also contained the same 3 CD184 and CD73 factions. As with the H1 hESC-derived fractions, HE as measured by EHT, as well as lymphoid and myeloid/erythroid potential segregated to the *R1C*-GFP-derived CD73$^-$CD184$^-$ fraction (Supplementary Fig 5e-g). Taken together,

these findings demonstrate that day 8 $CD34^+$ definitive HE can be distinguished from VE based on expression of CD73 and CD184.

Murine HE cells lack expression of CD184 and CD73 *in vivo*

To determine if HE *in vivo* displays a $CD184^-CD73^-$ phenotype, we next analysed the *Runx1*$^+$ $CD31^+$ population in the aorta-gonad-mesoneprhos (AGM) and yolk sac (YS), of E8.5, E9.5 and E10.5 *Runx1*-GFP mouse embryos for expression of these markers. Co-expression of *Runx1* and CD31 marks HE in both tissues at these stages[25]. Neither the AGM- or YS-derived HE cells expressed CD184 or CD73 (Supplementary Fig. 6a-d) indicating that HE *in vivo* can also be characterized as a $CD184^-CD73^-$ progenitor.

CD184 and CD73 expression distinguishes HE from arterial and venous VE

Quantitative RT-PCR analyses showed that the hESC-derived $CD34^+CD43^-$CD73-$CD184^-$ fraction expressed the highest levels of early haematopoietic genes including *RUNX1C*, *MYB*, and *TAL1*, while arterial endothelial genes, such as *EPHRINB2* and *DLL4*[26], were detected at highest levels in the $CD73^{med}CD184^+$ fraction (Fig. 4f). Conversely, expression of *NR2F2*, the master regulator of venous endothelium development[27], was highest in the $CD73^{hi}CD184^-$ fraction (Fig. 4f). These patterns suggest that the expression of CD184 and CD73 can be used to separate the $CD34^+$ VE population into distinct fractions with arterial and venous potential.

To confirm that the $CD73^{med}CD184^+$ and $CD73^{hi}CD184^-$ populations represent distinct endothelial cell types, we transplanted them subcutaneously in a Matrigel plug into immunocompromised NOD.Cg-*Prkdc*^{scid} *Il2rg*^{tm1Wjl}/SzJ **(**NSG) mice. Four weeks following transplantation, hESC-derived vascular structures comprised of human $CD31^+$ cells were detected in the grafts from both populations (Fig. 5a). The vessels generated from the $CD73^{med}CD184^+$ cells were considerably larger than those derived from the $CD73^{hi}CD184^-$ cells. Additionally they had larger numbers of α-SMA^+ cells associated with them, likely reflecting the recruitment of vascular smooth muscle cells (Fig. 5a,b). The $CD31^+$ cells in these grafts did not express the venous endothelial marker Ephrin Receptor B4 (EPHB4) (Fig. 5c). These characteristics suggest that the $CD73^{med}CD184^+$-derived structures represent arterial vessels. The smaller vessels derived from the $CD73^{hi}CD184^-$ cells expressed EPHB4 indicative of developing venous vasculature (Fig. 5d). Autofluorescent erythrocytes were detected in the lumen of both types of vessels, demonstrating integration in the vasculature network of the host (Fig. 5e,f).

Studies in different model organisms have shown that Notch and mitogen-activated protein kinase (MAPK) signalling promote the arterial fate whereas signalling through the phosphoinositide 3-kinase (PI3K) pathway supports venous development[27, 28]. To determine if these pathways regulate development of the $CD73^{med}CD184^+$ and $CD73^{hi}CD184^-$ populations, we used a HES2 hESC line containing a tamoxifen (4-OHT) responsive NOTCH1 intracellular domain (Hes2-ICN1-ER™) to activate the NOTCH pathway and the small molecules LY294002 and PD0325901 to inhibit the PI3K and MEK/ERK pathways respectively. Induction of NOTCH or inhibition of PI3K between days 3 and 8 of differentiation led to a significant increase in the size of the $CD73^{med}CD184^+$ arterial

population (Fig. 5g). The reverse pattern was observed following the inhibition of NOTCH with GSI or MEK/ERK with PD0325901 as addition of these molecules led to an increase in the size of the $CD73^{hi}CD184^{-}$ venous population. Collectively these observations indicate that hPSC-derived $CD73^{med}CD184^{+}$ arterial and $CD73^{hi}CD184^{-}$ venous fates are regulated by the same pathways that regulate these fates in the embryo.

In addition to decreasing the size of the arterial fraction, NOTCH inhibition also led to a reduction in the size of the $CD73^{-}CD184^{-}$ fraction (Fig 5g). Although our studies above showed that addition of GSI between days 3 and 8 did not completely block haematopoietic development (Fig. 3b-c), it is possible that this manipulation of NOTCH signalling during this stage led to some reduction of haematopoietic potential. LDA analysis of T cell progenitors revealed that inhibition of NOTCH signalling between days 3 and 8 of differentiation did not significantly affect T cell progenitor frequency within the $CD34^{+}CD73^{-}CD184^{-}$ fraction. Although NOTCH inhibition reduced the size of the $CD34^{+}CD73^{-}CD184^{-}$ fraction, it also increased the size of the CD34 population. As a consequence, the percentage of $CD34^{+}CD73^{-}CD184^{-}$ cells and T cell progenitors generated in the total EB population did not differ between GSI treated and control cultures (Fig. 5h,i). Activation of NOTCH signalling in Hes2-ICN1-ER™-derived cells by 4-OHT treatment between days 3 and 8 of differentiation did not alter the size of the total CD34 population, the size of the $CD34^{+}CD73^{-}CD184^{-}$ fraction or the frequency of T cells progenitors within the $CD34^{+}CD73^{-}CD184^{-}$ fraction compare to the control. These findings confirm that manipulation of the NOTCH pathway between days 3 and 8 of differentiation does not significantly impact the generation of the HE lineage.

HE cells lack expression of the endothelial progenitor marker DLL4

To further characterize the progenitor potential of the $CD73^{-}CD184^{-}$ fraction, we carried out a clonal analyses under EHT culture conditions. Out of 384 cells analysed, 83 generated progeny (Fig. 6a) and, of these, 10 (3% of starting) displayed HE potential and underwent the EHT to generate round $CD45^{+}$ haematopoietic cells (Fig. 6b). The remaining 73 (20%) gave rise to adhesive $CD144^{+}$ endothelial cells (Fig. 6c). Haematopoietic and endothelial cells were never detected in the same clone. Wells containing both cell types were, however, observed when larger numbers (10) of $CD73^{-}CD184^{-}$ cells were plated (Fig. 6d), confirming that the conditions support the development of both lineages together. Single $CD73^{med}CD184^{+}$ and $CD73^{hi}CD184^{-}$ cells gave rise to only $CD144^{+}$ endothelial progeny, at cloning frequencies of 20-25%. Together, these findings demonstrate that the $CD73^{-}CD184^{-}$ fraction contains both HE and VE progenitors further indicating that they represent distinct lineages. Additionally, they show that HE is haematopoietic restricted, as these progenitors did not give rise to endothelial progeny.

We next sought to determine the heterogeneity in the $CD73^{med}CD184^{+}$ and $CD73^{hi}CD184^{-}$ and $CD73^{-}CD184^{-}$ populations by analysing the expression of *MYB* (haemogenic), *EFNB2* (arterial) and *NR2F2* (venous) at the single cell level. These analyses revealed that 71% of the $CD73^{med}CD184^{+}$ cells expressed only the arterial marker *EFNB2* whereas 75% of the $CD73^{hi}CD184^{-}$ cells expressed the venous marker *NR2F2*, indicating little contamination between the cell types (Fig. 6e). A subpopulation (21%) of the $CD73^{hi}CD184^{-}$ cells (5 out

18 cells) coexpressed the arterial and venous marker, a pattern that has been observed during the formation of the major vessels in the mouse embryo[29]. As expected, the $CD73^{-}CD184^{-}$ population contained *MYB*-expressing HE (15%, 6 out 40) as well as vascular progenitors as demonstrated by the presence of cells that express either *NR2F2* or *EFNB2* (in both cases 10%, 4 out of 40 cells).

To enrich for HE, we next analysed the $CD34^{+}CD73^{-}CD184^{-}$ fraction for expression of the NOTCH ligand DLL4 that is found on VE progenitors early in development[30]. As shown in Figure 7a, both $DLL4^{-}$ and $DLL4^{+}$ cells were detected. The percentage of $DLL4^{+}$ cells within the $DLL4^{+}$ fraction varied between experiments and ranged from 28% to 79%, (51% ± 7, mean ± SEM, n=6, independent). Gene expression analysis showed that *RUNX1C*, *MYB* and *GATA2* were expressed at significantly higher levels in the $DLL4^{-}$ than in the $DLL4^{+}$ cells (Fig. 7b). Clonal analysis revealed that the $DLL4^{-}$ subfraction was enriched for HE as 70% of the cells that formed a clone in the EHT assay (176 out of 480) generated only haematopoietic cells (Fig. 7c). The remaining 30% gave rise to only endothelial progeny. LDA analyses revealed a T cell progenitor frequency of 1/11 (ranging from 1/1 to 1/30, n=4, independent) in the $DLL4^{-}$ fraction. The $DLL4^{+}$ fraction, by contrast, was enriched in vascular potential, as 89% of the cells that formed a clone (111 out of 480) were endothelial restricted, whereas only 11% showed haematopoietic potential. T cell potential was detected only when 1000, or more, cells were plated. Together, these findings show that the $CD34^{+}CD73^{-}CD184^{-}DLL4^{-}$ fraction is highly enriched for HE and provide additional evidence that HE and VE progenitors represent distinct cell types that can be separated based on the expression of DLL4

$CD34^{+}CD73^{-}CD184^{-}DLL4^{-}$ HE generates multipotent haematopoietic progenitors

To determine if the T lymphoid, myeloid and erythroid lineages that develop from the HE derive from the same progenitor, single $CD73^{-}CD184^{-}DLL4^{-}$ cells were sorted directly onto OP9-DLL4 stroma and cultured for 7 days to promote EHT and haematopoietic expansion. The developing clones were harvested and cells from each were plated both into methylcellulose to measure erythroid/myeloid progenitors and onto fresh OP9-DLL4 stroma cells to monitor T lymphoid potential (Fig. 7d). Out of a total of 252 cells analysed, 68 displayed haematopoietic potential and of these 5 gave rise to lymphoid, myeloid and erythroid progeny. Eight cells showed lymphoid/myeloid potential, whereas the remainder differentiated to either lymphoid or myeloid and/or erythroid progeny (Fig. 7e,f). These findings demonstrate that a subset of $CD34^{+}CD73^{-}CD184^{-}DLL4^{-}$ HE cells are able to give rise to multiple blood cell lineages, likely through the generation of a multipotent hematopoietic progenitor during the EHT process.

Discussion

Although the close association of HE with the arterial vasculature in the developing embryo supports the hypothesis that these progenitors derive from the arterial endothelium[5, 31, 32], direct evidence establishing a progenitor-progeny relationship between the two populations is lacking. The findings in this study, demonstrating that arterial VE and definitive HE can be separated based on CD184 and CD73 expression and that clones derived from the

CD184^{-}CD73^{-}DLL4^{-} fraction contain either haematopoietic or endothelial cells provide strong evidence that these populations represent distinct lineages. These observations are consistent with those from a recent study showing that prospective HE cells isolated from murine AGM give rise to only haematopoietic or endothelial lineage, but never to both[33]. The finding in both studies that the haematopoietic clones do not contain endothelial cells strongly suggests that HE cells are haematopoietic restricted progenitors.

Our demonstration that the EHT of the CD34^{+} HE is NOTCH dependent, provides strong evidence that the derivative haematopoietic lineages represent the definitive program, as studies in other models have shown that definitive, but not primitive haematopoiesis requires Notch signalling[34]. Although this requirement for Notch signalling for definitive hematopoiesis is well established, it has remained unclear as to whether the the block in this program was due to an absence of HE or to its inability to undergo EHT. By manipulating the pathway at specific stages, we show for the first time that Notch signalling is not essential for generation of the CD34^{+} HE but rather appears to be required for the cells to progress though the EHT. A role for Notch signalling at the EHT stage is supported by recent findings in the zebrafish, that showed a cell-autonomous requirement for this pathway for the generation of HSC progenitors just prior their emergence from the aortic floor[35].

With the high frequency of HE in the CD73^{-}CD184^{-}DLL4^{-} fraction, we were able to demonstrate that a subpopulation of these progenitors are able to generate lymphoid, erythroid and myeloid progeny. Our interpretation of these findings is that following the EHT, these HE cells generate a multipotent hematopoietic progenitor that may represent the equivalent of the HSC precursor identified in the mouse embryo[36]. The identification of this multipotent progenitor, in particular its erythroid potential, rules out the possibility that our T cell assays are only detecting the equivalent of the immune-restricted progenitors found during mouse embryonic development prior to the emergence of the HSC[37, 38].

In summary, the findings from our study support a model (Fig. 7g) in which HE is characterized as a CD184^{-}CD73^{-}DLL4^{-} haematopoietic restricted progenitor that is specified as a lineage distinct from the VE at the mesoderm stage of development. Following a NOTCH dependent EHT, we propose that the HE gives rise to CD45^{+} multipotent progenitors that represent the HSC precursor stage of haematopoietic development. The hPSC-derived HE and the multipotent haematopoietic progenitors provide target populations for further investigating the pathways that regulate the generation of HSCs *in vitro*.

Methods

Maintenance and differentiation of human ES cells

The hESC lines H1, Hes2-ICN1-ER™ and HES3-*RUNX1C* $^{GFP/w}$ -EGFP were maintained on irradiated mouse embryonic fibroblasts in hESC media as described previously[2]. For differentiation, hESCs were cultured on Matrigel-coated plasticware (BD Biosciences) for 24 hours, followed by embryoid body generation, as described previously[2]. Briefly, the undifferentiated hESCs were dissociated with Tryp-LE (GIBCO) treatment, followed by scraping. Aggregates were resuspended in StemPro-34 (Invitrogen), supplemented with

penicillin/streptomycin (10 ng/mL), L-glutamine (2mM), ascorbic acid (1mM), monothioglycerol (MTG, 4×10^{-4}M; Sigma), transferrin (150 μg/mL) (referred to as "supplemented StemPro-34") and BMP-4 (10 ng/mL), and cultured in 6-well low-cluster plates (Corning) in a volume of 2 mL per well. Following 24 hours, bFGF was added to a final concentration of 5ng/mL. At day 2, the developing EBs were harvested, washed and resuspended in supplemented StemPro-34 with BMP-4, bFGF and either CHIR99021 (3 μM, Stemgent), IWP2 (3μM, Tocris Bioscience) or Activin-A (1ng/ml) as indicated. After 24 hours, the EBs were again harvested and resuspended in supplemented StemPro-34 containing VEGF (15 ng/mL), bFGF (5 ng/mL), IL-6 (10 ng/mL) and IL-11 (5 ng/mL) and cultured for 48 hours. At this stage, the EBs were fed with 2ml of the same media containing also SCF (50 ng/mL final), IGF-1 (25 ng/mL final) and EPO (2 U/mL final) and cultured until day 8. Cultures were maintained in a 5% CO_2/5% O_2/90% N_2 environment. All recombinant factors are human and were purchased from R&D Systems. Where indicated 4-OHT (1 μM, Sigma), GSI (L-685,458, 10 μM, R&D Systems) PI3Ki (LY294002, 10 μM R&D System), MEKi (PD0325901, 1 μM, Stemgent) were included.

Generation of targeted hESCs

The ICN1ER-IRES-Puro donor vector comprised the intracellular domain of NOTCH1 fused to a modified estrogen receptor binding domain (ICN1-ER) flanked by two incompatible loxP sites, wild-type loxP and loxP2272, along with an internal ribosome entry site (IRES) and puromycin resistance gene (Puro). The R26.RFP hESC line[39], containing the RFP (red fluorescent protein) reporter flanked with the aforementioned loxP sites targeted to the human ROSA26 locus, was electroporated with a Cre expression vector along with the ICN1ER-IRES-Puro donor vector. Successfully targeted Hes2-NICD-ER™ cells, in which the ICN1-ER cDNA replaced the RFP coding sequences by means of recombination-mediated cassette exchange, were selected by puromycin treatment (1ug/ml, Sigma).

The generation and characterization of the HES3-*RUNX1C* $^{GFP/w}$–EGFP reporter hESC line (*R1C*-GFP) is summarized in Supplementary Fig. 2 and will be described more fully elsewhere. Briefly, as shown in Supplementary Fig. 2a, *RUNX1C* targeting vectors comprised a 5' homology arm, sequences encoding GFP, a loxP flanked antibiotic resistance cassette with a PGK promoter driving either neomycin phosphotransferase (PGKneo) or hygromycin resistance (PGKhygro) genes and a 3' homology arm. The homology arms were amplified by polymerase chain reaction (PCR) from HES3[40] genomic DNA. The GFP sequences were cloned in frame with the start codon of *RUNX1C* in exon 1, downstream of the distal promoter. Linearized vectors were electroporated into wild-type HES3 cells and targeted clones were identified by PCR screening. Correct targeting of the *RUNX1C* locus was verified by sequencing PCR-generated fragments encompassing the entire 5' and 3' homology regions. *RUNX1C*$^{GFP/w}$ clones were expanded and the loxP flanked antibiotic resistance cassettes were excised by transient transfection with a Cre-recombinase plasmid, pEFBOS-Cre-IRESPuro, as described [41]. Single cell sorted subclones were screened by PCR for the removal of the PGKNeo or PGKHyg selection cassettes. Targeted lines expressed surface markers of undifferentiated hESCs (Supplementary Fig. 2b), retained a normal karyotype (Supplementary Fig. 2c) and formed teratomas (Supplementary Fig. 2e-i) following injection of undifferentiated *RUNX1C*$^{GFP/w}$ hESCs under the kidney capsule of

NOD/SCID/IL2Rγ$^{-/-}$ mice as described below. The fidelity of the reporter was confirmed by demonstrating that expression of the *RUNX1C* isoform co-segregated with GFP expression.

Teratoma assay

Eight to ten week old male or female NSG mice were anaesthetised and injected under the kidney capsule with 1 × 10^6 undifferentiated *RUNX1C*$^{GFP/w}$ hESCs. Mice received post-operative analgesia to alleviate discomfort. Mice were euthanised humanely after 6 weeks or earlier if palpable tumours causing distress were present. Three mice were injected all of which developed teratomas. Tumours were fixed in paraformaldehyde containing solution, embedded in paraffin and sections stained with hematoxylin and eosin. This work was performed under the auspices of the Monash University animal ethics committee (approval number SOBSA-MIS-2009-107). No statistical method was used to predetermine sample size. The experiments were not randomized. The investigators were not blinded to allocation during experiments and outcome assessment.

Flow Cytometry and Cell Sorting

The following antibodies were used for these studies: CD34-APC (clone 8G12, 1:100), CD34-PE-CY7 (clone 4H11, 1:100), CD43-PE or FITC (clone 1G10, 1:30 and 1:10 respectively), CD4-PE-Cy7 (clone RPA-T4, 1:100), CD8-PE (clone RPA-T8, 1:30), CD45-APC-Cy7 or eFluor450 (clone 2D1, 1:50), CD56-APC (clone B159, 1:30), CD144-PE (clone 123413, 1:50), CD184-Brilliant Violet 421 (clone 12G5, 2:100), CD73-APC (clone AD2, 1:400), KDR (clone 89106, 1:7) and CD235a-APC (clone HIR2, 1:50). Most antibodies were purchased from BD Biosciences (San Diego, CA). The exceptions are CD34-PE-CY7 and CD144-PE that were purchased from eBioscience, CD184-Brilliant Violet 421 purchased from Biolegend and KDR purchased from R&D systems. Cells were sorted with FACSAria™II (BD) cell sorter at the Sick Kids/UHN Flow Cytometry Facility.

Endothelial-to-haematopoietic transition assay

Candidate cells (total CD34$^+$CD43$^-$, CD34$^+$CD43$^-$CD73^{hi}CD184$^-$, CD34$^+$CD43$^-$CD73^{med}CD184$^+$ or CD34$^+$CD43$^-$CD73$^-$CD184$^-$ cells) were aggregated overnight at a density of 2×10^5/ml in supplemented StemPro-34 media, containing TPO (30 ng/mL), IL-3 (30 ng/mL), SCF (100 ng/mL), IL-6 (10 ng/mL), IL-11 (5 ng/mL), IGF-1 (25 ng/mL), EPO (2 U/mL), VEGF (5 ng/mL), bFGF (5 ng/mL), BMP4 (10 ng/mL), Flt-3L (10 ng/mL), SHH (20 ng/mL), Angiotensin II (10 μg/L) and the chemical AGTR1 (angiotensin II receptor type I) blocker Losartan Potassium (100 μM). All recombinant factors are human and most were purchased from R&D Systems. The exceptions are Angiotensin II that was purchased from Sigma and EPO that was purchased from Jenssen-Cilag. Aggregates were then transferred onto thin-layer Matrigel coated plasticware where they were cultured for additional 4 to 6 days in the same media. Cultures were maintained in a 5% CO_2/5% O_2/90% N_2 environment. Cells were visualized using a Leica Imaging System.

OP9-DLL4 co-culture for T lineage differentiation

OP9 cells expressing Delta-like 4 (OP9-DLL4) were generated and described previously[2]. 0.5-20×10^4 candidate cells were added to individual wells of a 6-well plate containing OP9-DLL4 cells, and cultured in α-MEM supplemented with penicillin/streptomycin and 20% FBS, rhFlt-3L (5 ng/mL) and rhIL-7 (5 ng/mL). rhSCF (100 ng/mL) was added to the cultures for the first 5 days. Every five days co-cultures were transferred onto fresh OP9-DLL4 cells by vigorous pipetting and passaging through a 40μm cell strainer. Cells were analyzed by flow cytometry on the days indicated. Populations scored as positive yielded greater than 100 gated $CD45^+$ events.

Haematopoietic Colony Assay

Analysis of haematopoietic colony potential was performed by plating 0.1×10^4-1×10^4 cells in 1% methylcellulose containing specific cytokines as described in detail previously[2]. Colonies consisting of erythroid, erythroid/myeloid and myeloid (either macrophage or mast cell) cells were quantified after 14 days.

Multilineage Clonal Assay

Single $CD34^+CD73^-CD184^-DLL4^-$ cells were sorted directly into individual wells of a 96-well plate containing OP9-DLL4 cells, and cultured in α-MEM supplemented with penicillin/streptomycin and 20% FBS, rhTPO (30 ng/mL), rhIL11 (5ng/ml), rhFlt-3L (10 ng/mL), rhSCF (50 ng/mL), rhBMP4 (10 ng/mL) and rhIL-7 (5 ng/mL) for 7 days. At this stage, individual wells were trypsinized and half the cells transferred onto fresh OP9-DLL4 stroma for additional 21 days to measure T cell potential as described above, and the remaining half seeded into methylcellulose (as above: Hematopoietic Colony Assay) to evaluate erythro-myeloid potential.

Time-lapse and confocal microscopic imaging

Microscopic observations were obtained by using an Olympus Fluoview FV1000 confocal laser scanning microscope (Olympus America, Melville, NY.), with a PlanApo 60x oil immersion lens, numerical aperture 1.4. CD45-FITC was excited with a 473 nm diode laser (15mW), with an emission setting of 520 nm. The cKit PE was excited with a 559 nm diode laser (18 mW) with an emission setting of 567 nm. CD144 AlexaFluor647 was excited with a 635nm laser (20 mW) with an emission setting of668 nm. The Imaris software (Bitplane AG) was used for the 3D rendering. For the time-lapse experiments, cells were evaluated in a PECON environment chamber (PeCon GmbH) that maintains a temperature of 37 °C and a CO2 concentration of 5%. Time lapse images were taken every 10 min during a period up to 24h. Zeiss Apotome microscope (Zeiss Canada, Toronto, ON) and ZEN software suite (Carl Zeiss, version 2012) were used for the image acquisition. CD45 APC was excited with a Mercury light. The excitation setting was 592-650nm. The emission setting was a 665-735 nm. A transmitted light image was made at the same time as the fluorescent image. The cultures were imaged with a 20x Plan-Apochromat lens, N.A. 0.8.

Quantitative Real-time PCR

Total RNA was prepared with the RNAqueous RNA Isolation Kit (Ambion) and treated with RNase-free DNase (Qiagen). 100ng to 1ug RNA was transcribed into cDNA using random hexamers and Oligo (dT) with Superscript III Reverse Transcriptase (Invitrogen). Real-time quantitative PCR was performed on a MasterCycler EP RealPlex (Eppendorf). All experiments were carried out in triplicate QuantiFast SYBR Green PCR Kit (Qiagen). The oligonucleotide sequences are available upon request. Gene expression was evaluated as DeltaCt relative to control (*TBP*).

Thermo-Fast® 96 PCR Plate Non-Skirted 96-well PCR plates (Thermo Scientific) were used for the collection of single cells. Single cells were collected directly into 5 μL Lysis solution consisting of 5x VILO Reaction Mix (Invitrogen); 0.5% NP40 (Thermo Scientific); 0.4 units/μL RNaseOut (Invitrogen). Lysed cells were frozen on dry ice. In order to synthesize cDNA, the thawed plate of lysed cells was incubated for 90 s at 65 °C. Following this step, 1 μL of a mix containing 10x SuperMIX VILO (Invitrogen) and 1.2ug of T4 Gene 32 Protein (NEB) was added to each well. The plate was subjected to the following thermal protocol: 25 °C, 5 min; 42 °C, 30 min; 85 °C, 5 min; 4 °C, hold. At this point, the preamplification was performed as previously described[42], followed by the aforementioned qRT-PCR. For the single cell analyses, *ACTB* was analyzed as a control .

In vivo analyses of vascular progenitors

Between 0.2 and 0.5×10^6 $CD34^+CD43^-CD73^{med}CD184^+$ $CD34^+CD43^-CD73^{hi}CD184^-$ were mixed with 40ul of Matrigel and subcutaneously injected in the mammary fat pad of 12-weeks-old female NSG mice. Four weeks later, mice were sacrificed, the Matrigel plug dissected out and processed for paraffin sectioning. For immunostaining, the resulting sections were washed twice with, PBS and then blocked with 10% donkey serum in PBS/BSA 2% for 30-45 min. Following these step, the sections were incubated overnight at 4°C with the primary Ab. Human cells were detected by human-specific CD31 staining (rabbit, clone#9G11, R&D System, 1:50). Smooth muscle cells were analyzed following staining with smooth muscle α-actin (goat, clone E184, Abcam, 1:1000). Ephrin Receptor B4 expression was analyzed with a goat anti-EPHB4 antibody (goat, R&D System, 1:10). Incubation with these primary antibodies (Abs) was performed overnight at 4°C on sections previously blocked with 10% donkey serum in PBS/BSA 2% for 30-45 min. After staining, the cells were washed three times in PBS and incubated with a donkey anti-rabbit AlexaFluor 488 (1:800, Invitrogen, for hCD31) and a donkey anti-goat Cy3 (1:400, Jackson ImmunoResearch, for SMA or EPHB4) for 1h at room temperature. The cells were washed again (three times in PBS) and the nuclei were stained with DAPI diluted in PBS for 5 min at room temperature. The stained cells were visualized using an EVOS® FL Cell Imaging System (Life Technologies). All experiments with animals were performed according to the University Health Network Animal Resource Center's guidelines. No statistical method was used to predetermine sample size. The experiments were not randomized. The investigators were not blinded to allocation during experiments and outcome assessment.

Embryo generation and cell preparation and analysis

Timed matings of *Runx1*^{GFP} mice (*Runx1*^{tm4Dow})[43] were performed to generate embryos, with vaginal plug considered as embryonic day (E) 0.5. Embryos with 32–40 somite pairs were staged as E10.5. AGM and YS were disaggregated with collagenase, as previously described[44]. The following mouse Abs were used: CD31 PE-Cy7 (clone 390, eBioscience, 1:200), CD41-PerCP-eFluor710 (clone eBioMWReg30, eBioscience, 1:200), CD45-PerCP-Cy5.5 (clone 102, BD Pharmingen, 1:200), Ter119-eFlour450 (clone TER-119, eBioscience, 1:200), CD184-APC (clone 2B11, BD Pharmingen, 1:200), CD73-PE (clone eBioTY/11.8, eBioscience, 1:200). DAPI (Life Technologies) was used to exclude dead cells. No statistical method was used to predetermine sample size. The experiments were not randomized. The investigators were not blinded to allocation during experiments and outcome assessment.

Supplementary Material

Refer to Web version on PubMed Central for supplementary material.

Acknowledgements

We would like to thank the SickKids–UHN Flow Cytometry Facility for their expert assistance with cell sorting, in particular A. Khandani, Feng Xu at the Advanced Optical Microscopy Facility for the great help with the time-lapse and confocal imaging, and Dr. Sasan Zandi for assistance with single cell qRT-PCR. This work was supported by the National Institutes of Health grant U01 HL100395 to G.K., SR00002303 to N.S. and by the Canadian Institutes of Health Research grants MOP93569 and EPS 127882 to G.K Additional support to A.D. and C.M.S. was provided by the Magna-Golftown Post-Doctoral Fellowship and the McMurrich Post-Doctoral Fellowship, respectively. A.G.E and E.G.S are Senior Research Fellows of the National Health and Medical Research Council (NHMRC) of Australia. Their work was supported by Stem Cells Australia, the NHMRC and the Victorian Government's Operational Infrastructure Support Program.

References

1. Kaufman DS. Toward clinical therapies using hematopoietic cells derived from human pluripotent stem cells. Blood. 2009; 114:3513–3523. [PubMed: 19652198]
2. Kennedy M, et al. T lymphocyte potential marks the emergence of definitive hematopoietic progenitors in human pluripotent stem cell differentiation cultures. Cell reports. 2012; 2:1722–1735. [PubMed: 23219550]
3. Klimchenko O, et al. Monocytic cells derived from human embryonic stem cells and fetal liver share common differentiation pathways and homeostatic functions. Blood. 2011; 117:3065–3075. [PubMed: 21149635]
4. Takayama N, et al. Generation of functional platelets from human embryonic stem cells in vitro via ES-sacs, VEGF-promoted structures that concentrate hematopoietic progenitors. Blood. 2008; 111:5298–5306. [PubMed: 18388179]
5. Clements WK, Traver D. Signalling pathways that control vertebrate haematopoietic stem cell specification. Nature reviews. Immunology. 2013; 13:336–348. [PubMed: 23618830]
6. Bertrand JY, et al. Haematopoietic stem cells derive directly from aortic endothelium during development. Nature. 2010; 464:108–111. [PubMed: 20154733]
7. Boisset JC, et al. In vivo imaging of haematopoietic cells emerging from the mouse aortic endothelium. Nature. 2010; 464:116–120. [PubMed: 20154729]
8. Kissa K, Herbomel P. Blood stem cells emerge from aortic endothelium by a novel type of cell transition. Nature. 2010; 464:112–115. [PubMed: 20154732]

9. Rybtsov S, et al. Tracing the origin of the HSC hierarchy reveals an SCF-dependent, IL-3-independent CD43(−) embryonic precursor. Stem cell reports. 2014; 3:489–501. [PubMed: 25241746]
10. Sturgeon CM, Ditadi A, Awong G, Kennedy M, Keller G. Wnt signaling controls the specification of definitive and primitive hematopoiesis from human pluripotent stem cells. Nature biotechnology. 2014; 32:554–561.
11. Bertrand JY, Cisson JL, Stachura DL, Traver D. Notch signaling distinguishes 2 waves of definitive hematopoiesis in the zebrafish embryo. Blood. 2010; 115:2777–2783. [PubMed: 20107232]
12. Hadland BK, et al. A requirement for Notch1 distinguishes 2 phases of definitive hematopoiesis during development. Blood. 2004; 104:3097–3105. [PubMed: 15251982]
13. Kumano K, et al. Notch1 but not Notch2 is essential for generating hematopoietic stem cells from endothelial cells. Immunity. 2003; 18:699–711. [PubMed: 12753746]
14. Robert-Moreno A, Espinosa L, de la Pompa JL, Bigas A. RBPjkappa-dependent Notch function regulates Gata2 and is essential for the formation of intra embryonic hematopoietic cells. Development (Cambridge, England). 2005; 132:1117–1126.
15. Peeters M, et al. Ventral embryonic tissues and Hedgehog proteins induce early AGM hematopoietic stem cell development. Development (Cambridge, England). 2009; 136:2613–2621.
16. Robin C, Durand C. The roles of BMP and IL-3 signaling pathways in the control of hematopoietic stem cells in the mouse embryo. The International journal of developmental biology. 2010; 54:1189–1200. [PubMed: 20711995]
17. Zambidis ET, et al. Expression of angiotensin-converting enzyme (CD143) identifies and regulates primitive hemangioblasts derived from human pluripotent stem cells. Blood. 2008; 112:3601–3614. [PubMed: 18728246]
18. Yokomizo T, Dzierzak E. Three-dimensional cartography of hematopoietic clusters in the vasculature of whole mouse embryos. Development (Cambridge, England). 2010; 137:3651–3661.
19. Bee T, et al. Alternative Runx1 promoter usage in mouse developmental hematopoiesis. Blood cells, molecules & diseases. 2009; 43:35–42.
20. Choi KD, et al. Identification of the hemogenic endothelial progenitor and its direct precursor in human pluripotent stem cell differentiation cultures. Cell reports. 2012; 2:553–567. [PubMed: 22981233]
21. Rafii S, et al. Human ESC-derived hemogenic endothelial cells undergo distinct waves of endothelial to hematopoietic transition. Blood. 2013; 121:770–780. [PubMed: 23169780]
22. Uenishi G, et al. Tenascin C promotes hematoendothelial development and T lymphoid commitment from human pluripotent stem cells in chemically defined conditions. Stem cell reports. 2014; 3:1073–1084. [PubMed: 25448067]
23. Yamamizu K, et al. Convergence of Notch and beta-catenin signaling induces arterial fate in vascular progenitors. The Journal of cell biology. 2010; 189:325–338. [PubMed: 20404113]
24. Yurugi-Kobayashi T, et al. Adrenomedullin/cyclic AMP pathway induces Notch activation and differentiation of arterial endothelial cells from vascular progenitors. Arteriosclerosis, thrombosis, and vascular biology. 2006; 26:1977–1984.
25. Tober J, Yzaguirre AD, Piwarzyk E, Speck NA. Distinct temporal requirements for Runx1 in hematopoietic progenitors and stem cells. Development (Cambridge, England). 2013; 140:3765–3776.
26. Marcelo KL, Goldie LC, Hirschi KK. Regulation of endothelial cell differentiation and specification. Circulation research. 2013; 112:1272–1287. [PubMed: 23620236]
27. You LR, et al. Suppression of Notch signalling by the COUP-TFII transcription factor regulates vein identity. Nature. 2005; 435:98–104. [PubMed: 15875024]
28. Hong CC, Peterson QP, Hong JY, Peterson RT. Artery/vein specification is governed by opposing phosphatidylinositol-3 kinase and MAP kinase/ERK signaling. Current biology : CB. 2006; 16:1366–1372. [PubMed: 16824925]
29. Lindskog H, et al. Molecular identification of venous progenitors in the dorsal aorta reveals an aortic origin for the cardinal vein in mammals. Development (Cambridge, England). 2014; 141:1120–1128.

30. Benedito R, Duarte A. Expression of Dll4 during mouse embryogenesis suggests multiple developmental roles. Gene expression patterns : GEP. 2005; 5:750–755. [PubMed: 15923152]
31. Richard C, et al. Endothelio-mesenchymal interaction controls runx1 expression and modulates the notch pathway to initiate aortic hematopoiesis. Developmental cell. 2013; 24:600–611. [PubMed: 23537631]
32. Ciau-Uitz A, Wang L, Patient R, Liu F. ETS transcription factors in hematopoietic stem cell development. Blood cells, molecules & diseases. 2013; 51:248–255.
33. Swiers G, et al. Early dynamic fate changes in haemogenic endothelium characterized at the single-cell level. Nature communications. 2013; 4:2924.
34. Bigas A, Robert-Moreno A, Espinosa L. The Notch pathway in the developing hematopoietic system. The International journal of developmental biology. 2010; 54:1175–1188. [PubMed: 20711994]
35. Kim AD, et al. Discrete Notch signaling requirements in the specification of hematopoietic stem cells. The EMBO journal. 2014; 33:2363–2373. [PubMed: 25230933]
36. Godin I, Garcia-Porrero JA, Dieterlen-Lievre F, Cumano A. Stem cell emergence and hemopoietic activity are incompatible in mouse intraembryonic sites. The Journal of experimental medicine. 1999; 190:43–52. [PubMed: 10429669]
37. Boiers C, et al. Lymphomyeloid contribution of an immune-restricted progenitor emerging prior to definitive hematopoietic stem cells. Cell stem cell. 2013; 13:535–548. [PubMed: 24054998]
38. Luc S, et al. The earliest thymic T cell progenitors sustain B cell and myeloid lineage potential. Nature immunology. 2012; 13:412–419. [PubMed: 22344248]
39. Irion S, et al. Identification and targeting of the ROSA26 locus in human embryonic stem cells. Nature biotechnology. 2007; 25:1477–1482.
40. Richards M, Fong CY, Chan WK, Wong PC, Bongso A. Human feeders support prolonged undifferentiated growth of human inner cell masses and embryonic stem cells. Nature biotechnology. 2002; 20:933–936.
41. Davis RP, et al. A protocol for removal of antibiotic resistance cassettes from human embryonic stem cells genetically modified by homologous recombination or transgenesis. Nature protocols. 2008; 3:1550–1558. [PubMed: 18802436]
42. Livak KJ, et al. Methods for qPCR gene expression profiling applied to 1440 lymphoblastoid single cells. Methods. 2013; 59:71–79. [PubMed: 23079396]
43. Lorsbach RB, et al. Role of RUNX1 in adult hematopoiesis: analysis of RUNX1-IRES-GFP knock-in mice reveals differential lineage expression. Blood. 2004; 103:2522–2529. [PubMed: 14630789]
44. North TE, et al. Runx1 expression marks long-term repopulating hematopoietic stem cells in the midgestation mouse embryo. Immunity. 2002; 16:661–672. [PubMed: 12049718]

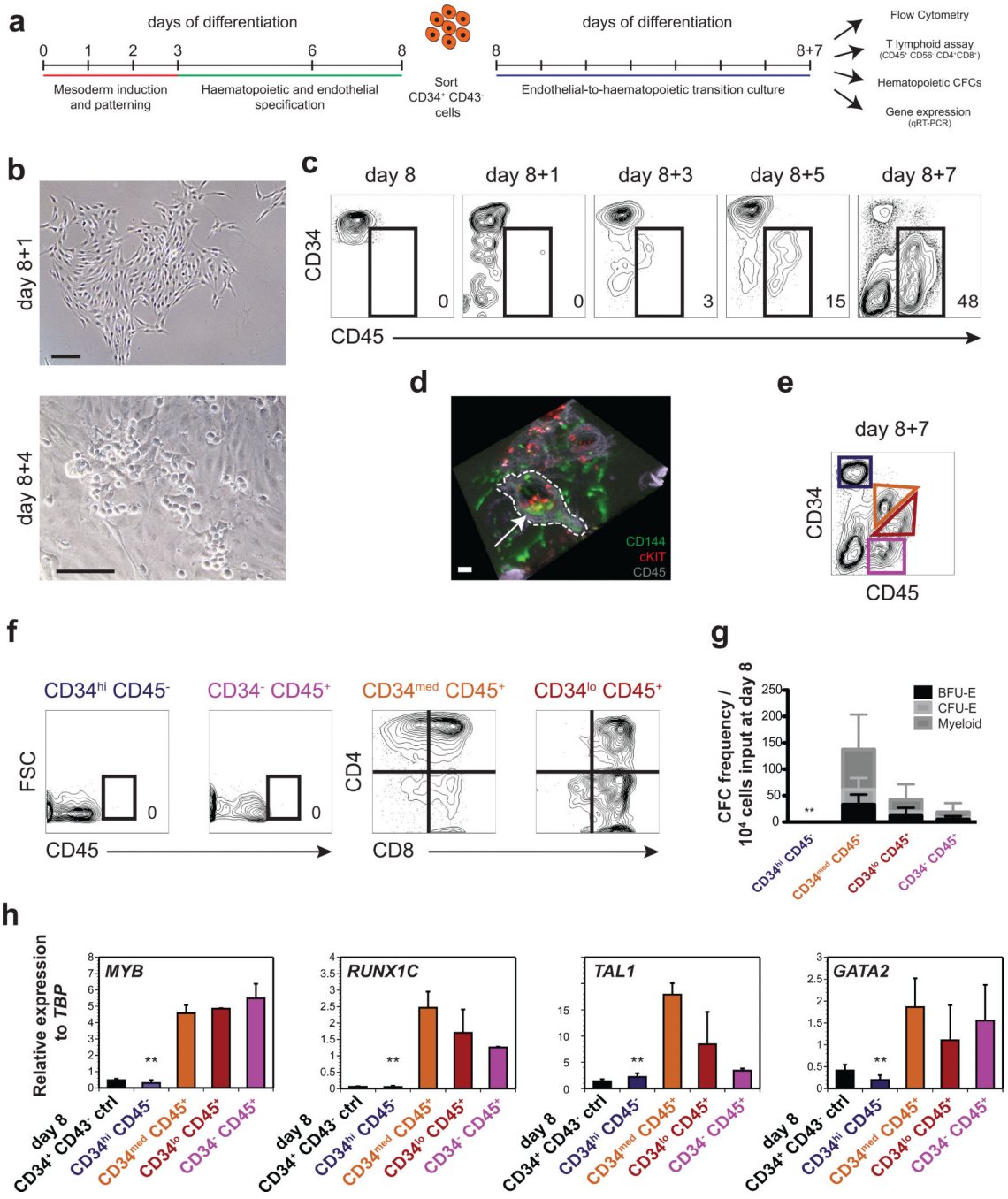

Figure 1. Characterization of hPSC-derived definitive haemogenic endothelium

a, Experimental scheme. $CD34^{+}CD43^{-}$ cells were isolated from embryoid bodies at day 8 of differentiation, reaggregated overnight in serum-free media supplemented with haematopoietic cytokines and then cultured for additional 6 days onto Matrigel-coated plates in the presence of haematopoietic cytokines to promote the endothelial-tohaematopoietic transition (EHT). This stage is referred to as the EHT culture. Following the EHT culture, the cells were assayed as indicated. **b,** Photomicrograph of day 8 $CD34^{+}$ $CD43^{-}$ -derived cells following 1 (upper) and 4 days (lower) of EHT culture. Non-adherent (haematopoietic)

cells are visible in the day 4 cultures. Scale bars: 100 μm. **c,** Representative flow cytometric analysis of the frequency of $CD34^+$ and $CD45^+$ cells in the day 8 $CD34^+$-derived populations at the indicated days of EHT culture. **d,** Visualization of emerging round haematopoietic cells in EHT cultures by confocal imaging. Cells were stained for the endothelial marker CD144 (in green), the haematopoietic marker CD45 (in gray) and the EHT marker cKIT (in red). Scale bar: 5 μm. Dashed line demarcates a cell coexpressing CD144, CD45 and cKIT (white arrow). **e,** Gating strategy used to define the different CD34/CD45 fractions in the $CD34^+$-derived population following 7 days of EHT culture. **f,** T cell potential of the different CD34/CD45 fractions indicated in **e** measured by the development of $CD4^+CD8^+$ cells within a $CD45^+CD56^-$ gate following culture on OP9-DLL4 stromal cells for 24 days. **g,** Haematopoietic colony-forming potential of the different CD34/CD45 fractions indicated in **e** generated following 7 days of EHT culture of day 8 $CD34^+CD43^-$ cells. $n = 4$, independent experiments. (Mean ± SEM). ** ANOVA $p = 0.002$. BFU-E: progenitors that generate large segmented erythroid colonies, CFU-E: progenitors that give rise to small erythroid colonies, Myeloid: includes macrophage and mast cell progenitors. **h,** qRT-PCR analysis of *MYB*, *RUNX1C*, *TAL1* and *GATA2* expression in the different CD34/CD45 fractions isolated as in **e**. The day 8 $CD34^+CD43^-$ population prior to culture is included as a control (ctrl). Cells were derived from H1 hESCs. $n = 4$, independent experiments. (Mean ± SEM). ** ANOVA $p < 0.0001$. Images in **b** and plots in **c** are representative of 6 independent experiments, in **f** of 3 independent experiments.

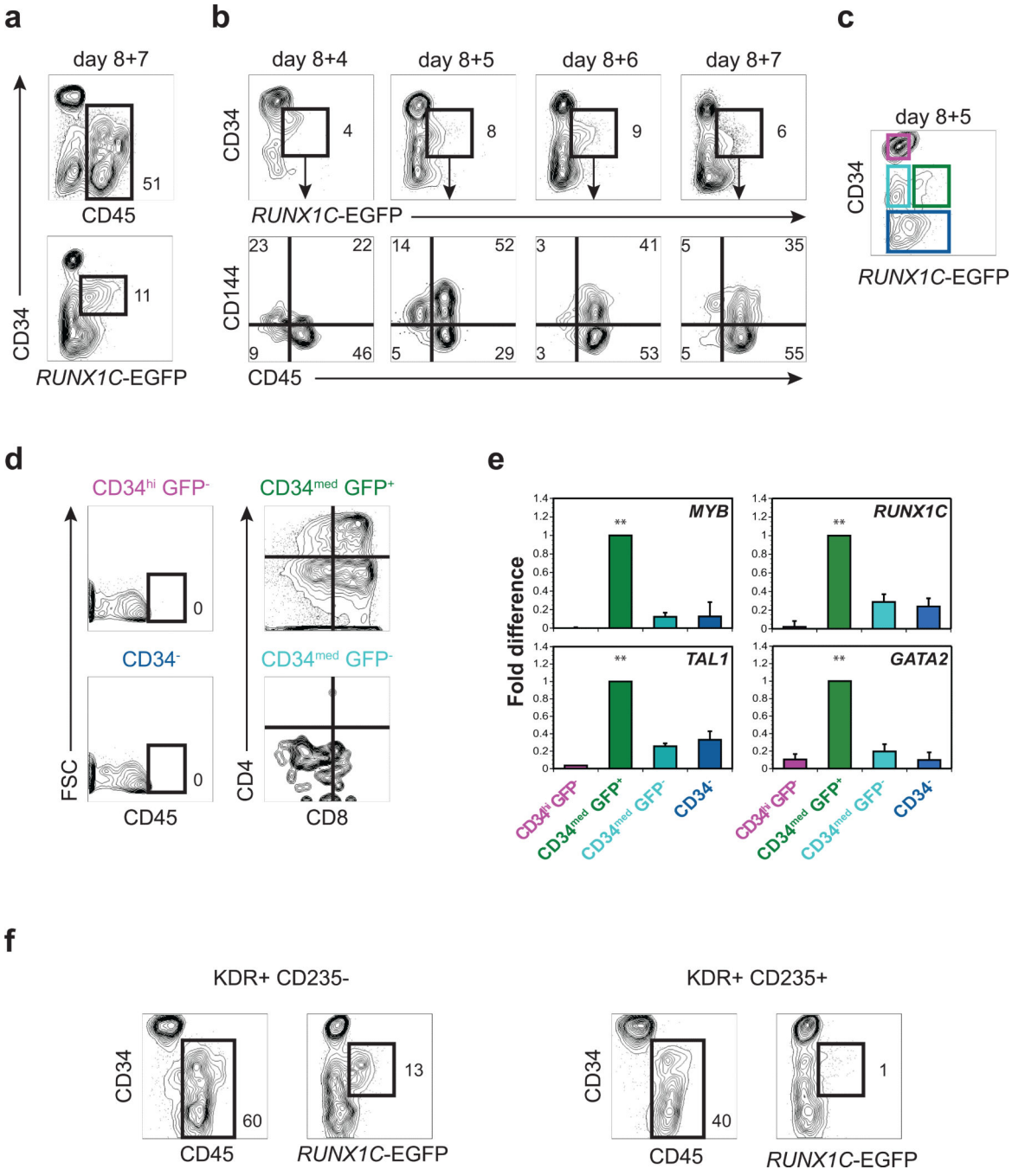

Figure 2. *RUNX1C*-EGFP is expressed during the EHT of the definitive haemogenic endothelium

a, Representative flow cytometric analysis of the frequency of $CD45^+$ cells (upper panel) and $CD34^+$ *RUNX1C-EGFP*$^+$ cells (lower panel) in the day 8-derived population following 7 days of EHT culture. **b,** Representative flow cytometric analysis of the frequency of $CD144^+$ and $CD45^+$ cells (lower panels) in the $CD34^+$*RUNX1C*-$EGFP^+$ fraction (upper panels) generated at the indicated times of EHT culture of day 8 $CD34^+CD43^-$ cells. **c,** Gating strategy used for the isolation of the $CD34^+$ and *RUNX1C*-$EGFP^+$ fractions in the $CD34^+$ -derived population following 5 days of EHT culture. **d,** T cell potential of the

different CD34/CD45 fractions (indicated in **c**) measured by the development of $CD4^+CD8^+$ cells within a $CD45^+CD56^-$ gate following culture on OP9-DLL4 stromal cells for 24 days. **e,** qRT-PCR analysis of *MYB*, *RUNX1C*, *TAL1* and *GATA2* expression in the different CD34/*RUNX1C*-EGFP fractions. $n = 3$, independent experiments. (Mean ± SEM). ** ANOVA *MYB*, *RUNX1C*, *GATA2* $p < 0.0001$, *TAL1* $p = 0.0003$. **f,** Representative flow cytometric analysis of the frequency of $CD34^+$ $CD45^+$ and $CD34^+$ *RUNX1C*-$EGFP^+$ cells generated after 7 days in EHT culture from $KDR^+CD235a^-$ (left panels) and $KDR^+CD235a^+$ (right panels) -derived $CD34^+CD43^-$ cells. Plots in **a** are representative of 5 independent experiments, in **b**, **d** and **f** of 3 independent experiments.

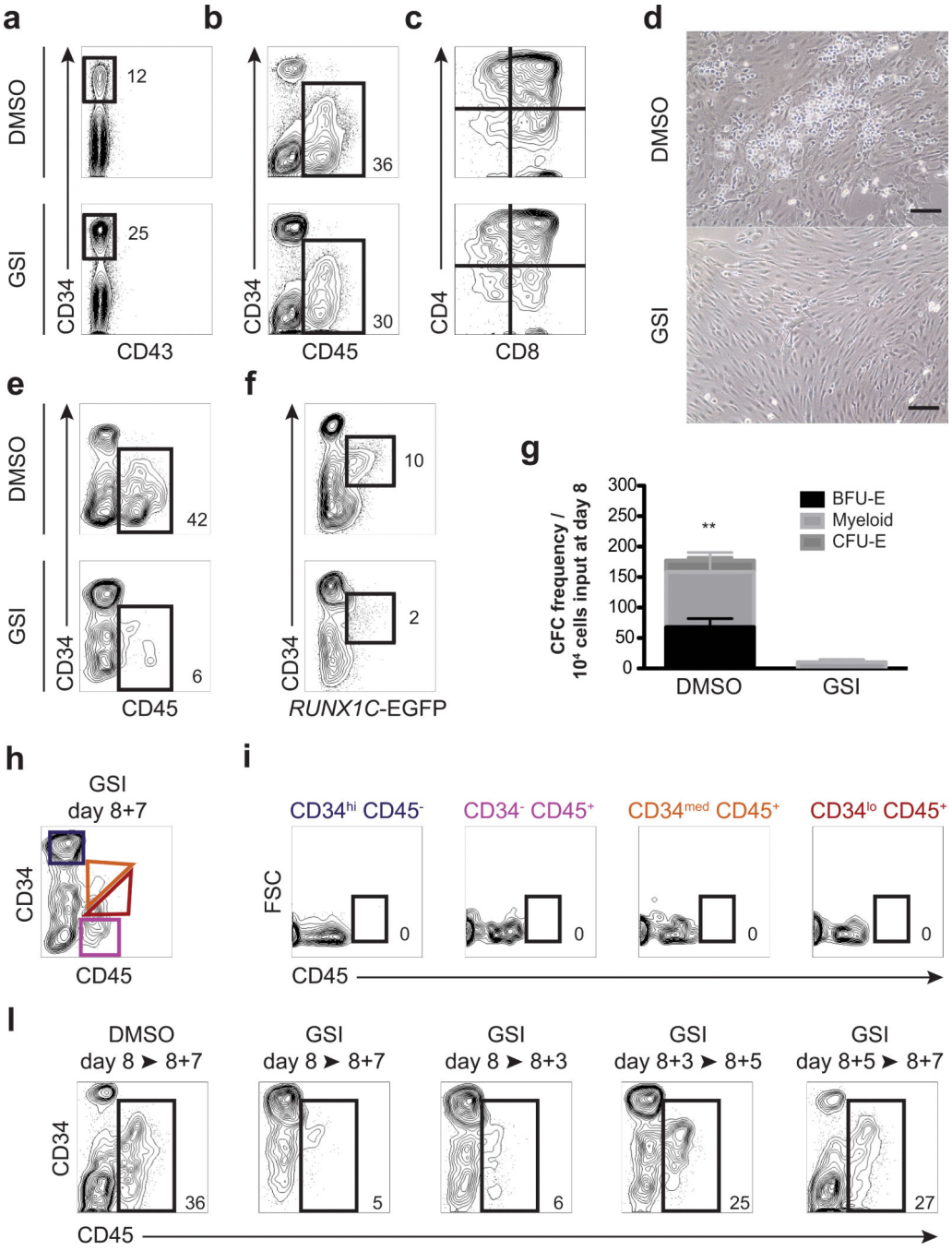

Figure 3. Haematopoietic specification of definitive haemogenic endothelium is Notch-dependent

a, Representative flow cytometric analysis of the frequency of $CD34^+$ $CD43^-$ cells in DMSO (upper panel) or GSI (lower panel) treated day 8 EBs generated from H1 ESCs. GSI or DMSO was added to the cultures every 60 hours from day 3 to 8 of differentiation. **b,** Representative flow cytometric analysis of the frequency of $CD34^+$ and $CD45^+$ cells in populations following 7 days of EHT culture of $CD34^+CD43^-$ cells isolated from DMSO (upper panel) or GSI (lower panel) treated EBs. **c,** T cell potential of $CD34^+CD43^-$ cells isolated from DMSO (upper panel) or GSI (lower panel) treated EBs measured by the

development of $CD4^+$ $CD8^+$ cells within a $CD45^+$ $CD56^-$ gate following culture on OP9-DLL4 stromal cells for 24 days. **d,** Photomicrograph of day 8 $CD34^+CD43^-$ -derived populations following addition of either DMSO or GSI to the EHT culture. Cells were analysed following 7 days of EHT culture in the presence of either DMSO or GSI. Emerging semi-adherent (haematopoietic) cells were detected in the DMSO- (upper panel) but not the GSI- (lower panel) treated population. Scale bars: 100 μm. **e, f,** Representative flow cytometry analysis of the frequency of $CD34^+$ $CD45^+$ cells (**e**) or $CD34^+$*RUNX1C*$EGFP^+$ cells (**f**) in populations following 7 days of EHT culture of H1- and *R1C*-GFP-derived $CD34^+CD43^-$ cells respectively. DMSO or GSI was added throughout the 7-day culture period. **g,** Haematopoietic colony-forming potential of the H1 hESC-derived day 7 EHT population treated with either DMSO and GSI. n=3 independent experiments. (Mean ± SEM). Student's *t*-test, ** $p < 0.0001$. **h,** Gating strategy used for the isolation of the CD34/CD45 fractions from the population generated following 7 days of EHT culture of day 8 $CD34^+$ $CD43^-$ cells in the presence of GSI. **i,** T cell potential of the different CD34/CD45 fractions following 24 days of culture on OP9-DLL4 stromal cells. The lack of any $CD45^+$ cells indicates that GSI-treatment during the EHT culture inhibited T cell development. **l,** Representative flow cytometric analysis of the frequency of $CD34^+$ and $CD45^+$ cells in day 8 $CD34^+CD43^-$ -derived EHT populations treated for the indicated times with GSI. Cells were analysed at day 7 of culture. Images in **a**, **b**, **e** and **f** are representative of 6 independent experiments, in **c** and **i** of 3 independent experiments, in **l** of 4 independent experiments.

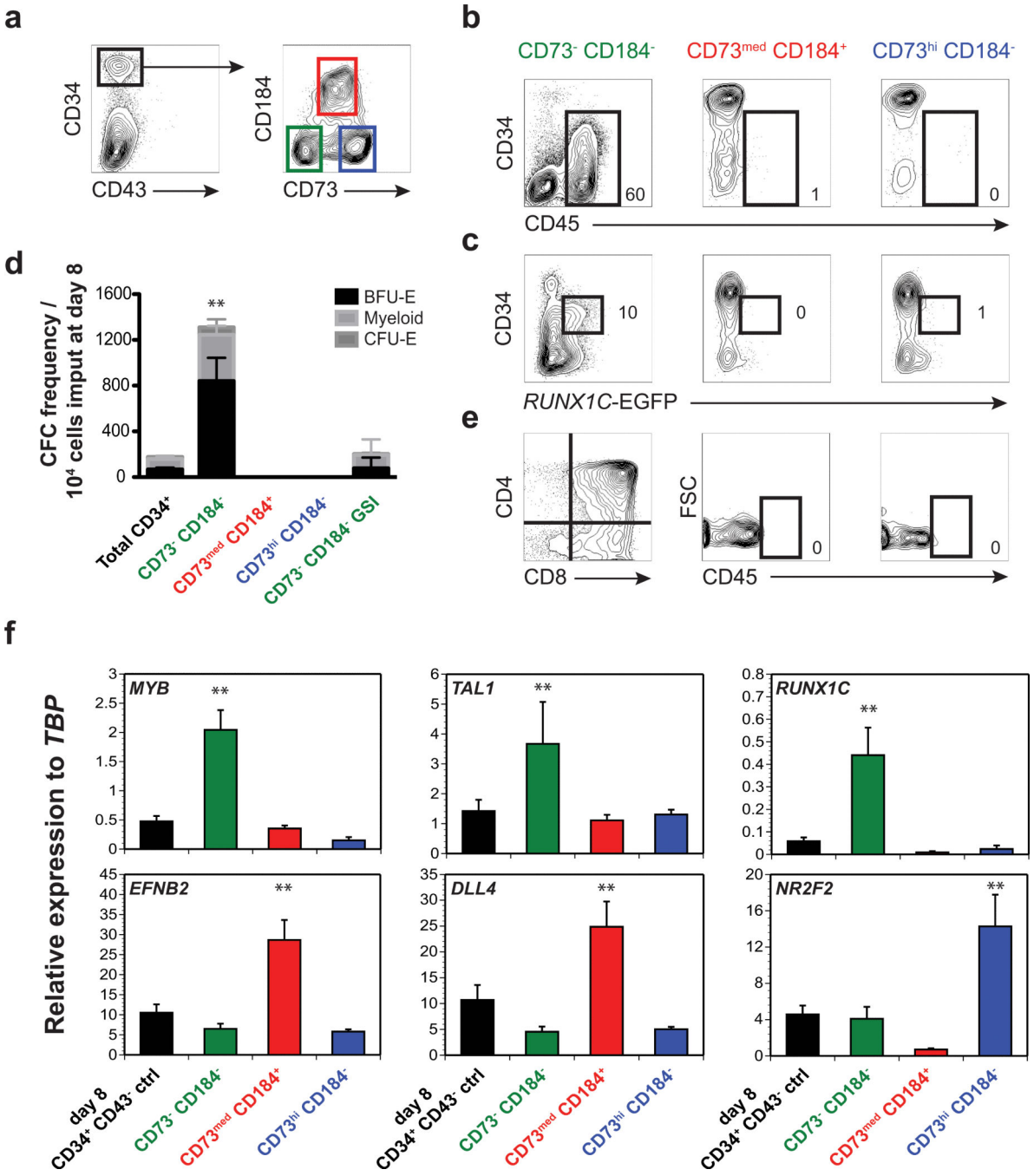

Figure 4. Expression of CD73 and CD184 distinguishes HE and VE in the day 8 CD34$^+$ CD43$^-$ population

a, Gating strategy used for the isolation of the CD184$^+$ and CD73$^+$ fractions from the day 8 CD34$^+$ CD43$^-$ population. **b,** Flow cytometric analyses of the frequency of CD34$^+$ and CD45$^+$ cells in populations generated from the 3 H1 hESC-derived CD184/CD73 fractions following 7 days of EHT culture. **c,** Representative flow cytometric analysis of the frequency of CD34$^+$ and RUNX1C-EGFP$^+$ cells generated from the 3 *R1C*-GFP hESC-derived CD184/CD73 fractions following 7 days of EHT culture. **d,** Haematopoietic colony-

forming potential of the CD184/CD73-derived populations following 7 days of EHT culture. The $CD73^{-}CD184^{-}$ -derived population was also treated with GSI during the EHT culture to evaluate NOTCH-dependency. $n = 3$, independent experiements. (Mean ± SEM). ** ANOVA $p < 0.0001$. **e,** T cell potential of the different H1-derived CD184/CD73 fractions measured by the development of $CD4^{+}$ $CD8^{+}$ cells following culture on OP9-DLL4 stromal cells for 24 days. **f,** qRT-PCR analysis of haematopoietic (*MYB*, *TAL1* and *RUNX1C*), arterial (*EFNB2*, *DLL4*) and venous gene (*NR2F2*) expression in the different CD184/CD73 fractions isolated from a day 8 $CD34^{+}$ EB population generated from H1 hESCs. $n = 5$, independent experiments. (Mean ± SEM). ** ANOVA *MYB*, *TAL1*, *EFNB2* and *NR2F2* $p < 0.0001$, *RUNX1C* $p = 0.0003$, *DLL4* $p = 0.0002$. Plots in **b** are representative of 6 independent experiments, in **c** and **e** of 3 independent experiments.

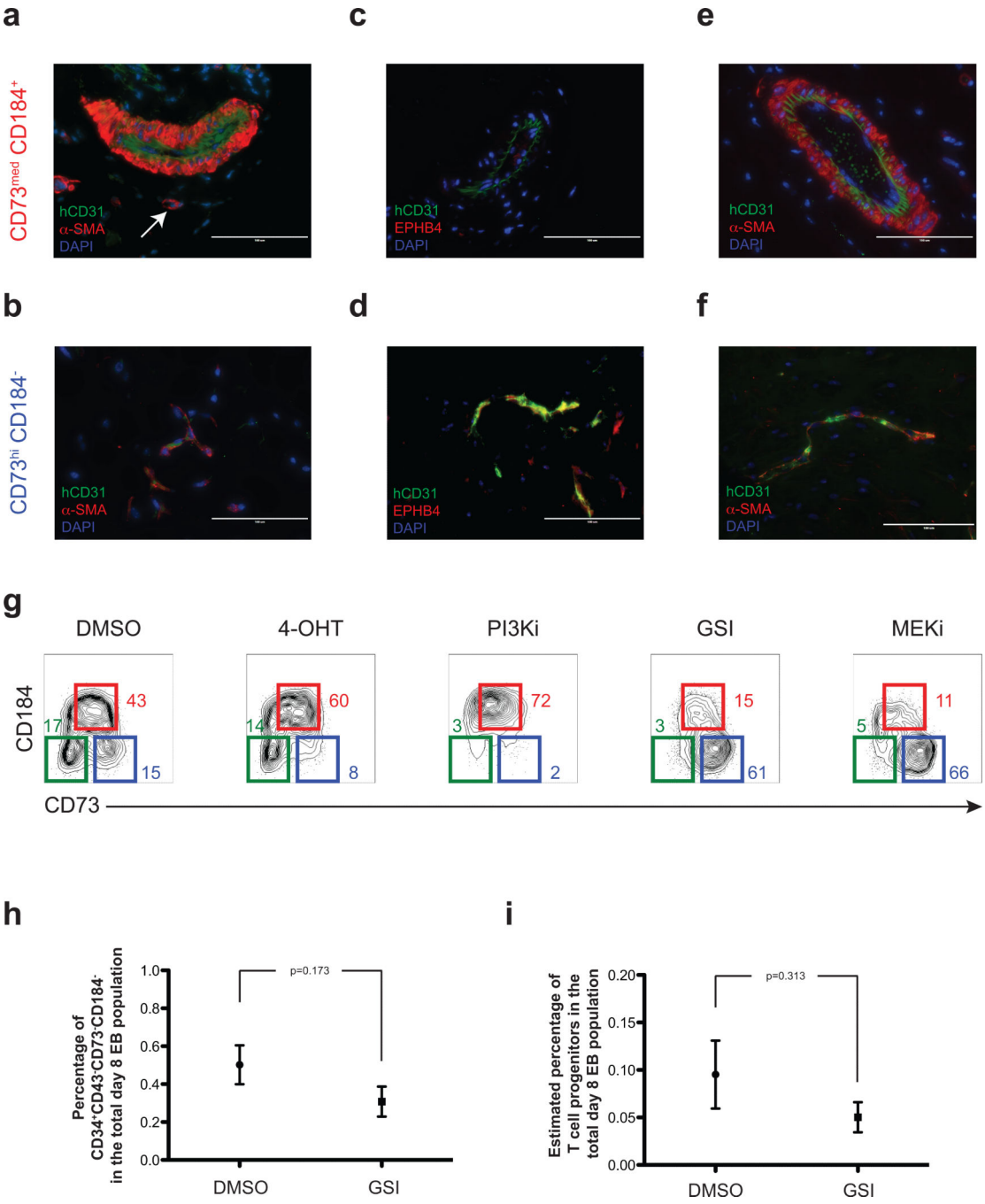

Figure 5. Engrafted CD73^{med}CD184^{+} and CD73^{hi}CD184^{-} cells maintain their vascular identity

a,c,e, photomicrographs of immunostained histological sections of vascular grafts derived from day 8 CD73^{med}CD184^{+} cells. **b, d, f,** photomicrographs of immunostained histological sections of vascular grafts derived from day 8 CD73^{hi}CD184^{-} cells. Green depicts the presence of human CD31^{+} cells and red the presence of α-smooth muscle actin (α-SMA)$^{+}$ cells (**a**, **b**, **e**, **f**) and eprhin receptor B4 (EPHB4)$^{+}$ cells (**c, d**). Nuclei are visualized by DAPI (blue) staining. The anti-CD31 antibody is specific for human CD31. Arrow indicates a murine vessel. * indicates autoflourescent red blood cells. Scale bars: 100 μm. **g,**

Representative flow cytometric analysis of the frequency of $CD184^+$ and $CD73^+$ cells in day 8 $CD34^+CD43^-$ populations generated from Hes2-ICN1-ER™ hESCs treated with DMSO, GSI (L-685,458 10μM), 4-OHT (1μM) , MEKi (PD0325901, 1μM) or PI3Ki (LY294002, 10μM) between day 3 and day 8 of differentiation. **h, i,** Graphs showing the total percentage of $CD34^+CD73^-CD184^-$ (**h**) and the estimated total percentage of T cell progenitors (**i**) in day 8 H1-derived total EB populations following DMSO or GSI treatment from day 3 to day 8 of differentiation (Student's *t*-test; p-value is shown. **h**, n=6 independent experiments; **i**, n=3, independent experiments). Images in **a-f** are representative of 4 mice from 4 independent experiments, in **g** of 3 independent experiments.

a

Cell Type	No. cells/well	Hematopoietic and Endothelial progeny	Hematopoietic progeny	Endothelial progeny
CD184^{+} CD73^{med}	1	0/192	0/192	51/192 (1:4)
CD184^{-} CD73^{hi}	1	0/192	0/192	42/192 (1:5)
CD184^{-} CD73^{-}	1	0/384	10/384 (1:38)	73/384 (1:5)
	10	18/96	1/96	66/96

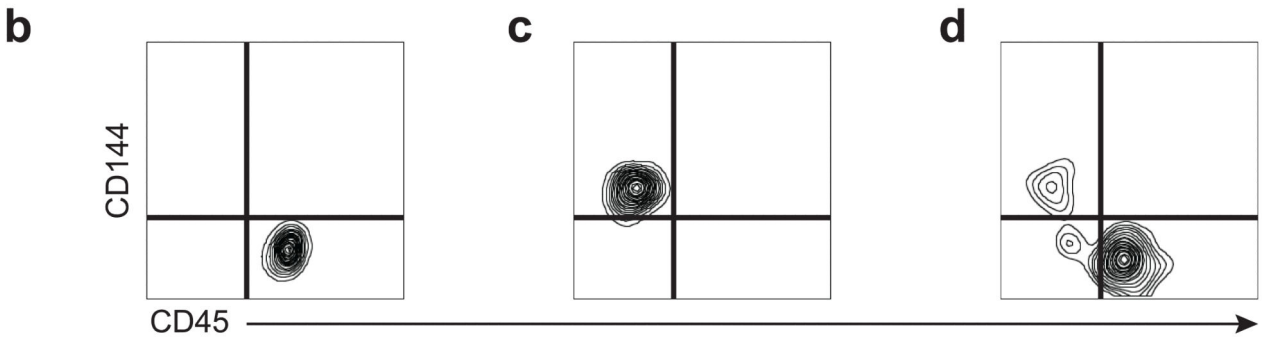

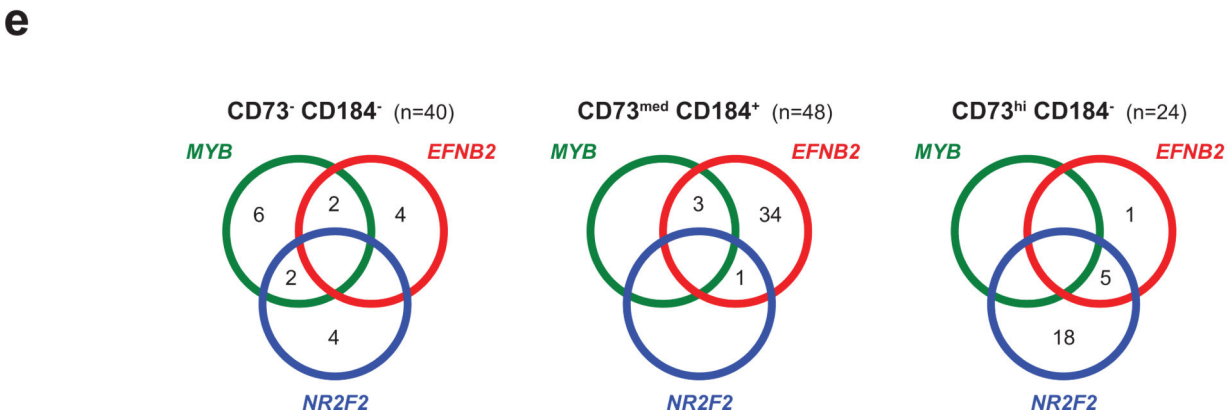

Figure 6. The CD34^{+}CD43^{-}CD73^{-}CD184^{-} fraction contains both HE and VE progenitors cells

a, Table showing the clonal analysis of the day 8 CD34^{+}CD184^{-}CD73^{-} EB population. Numbers indicate the positive wells containing haematopoietic and/or endothelial cells relative to the total number of wells seeded. Data are compiled from 4 independent experiments. **b-d,** Flow cytometric analysis of haematopoietic (**b**) and endothelial (**c**) clones and a representative well seeded with 10 cells, containing both haematopoietic and endothelial progeny (**d**). Data in **a-d** are compiled from 4 independent experiments. **e,** Venn diagram summarizing the number of cells in each of the indicated CD34^{+} fractions that

express the haematopoietic (*MYB*), arterial (*EFNB2*) and venous (*NR2F2*) genes measured by single cells qRT-PCR. The total number of cells from each fraction in which expression of housekeeping gene *ACTB* was detected is indicated in brackets. Data are compiled from 2 independent experiments.

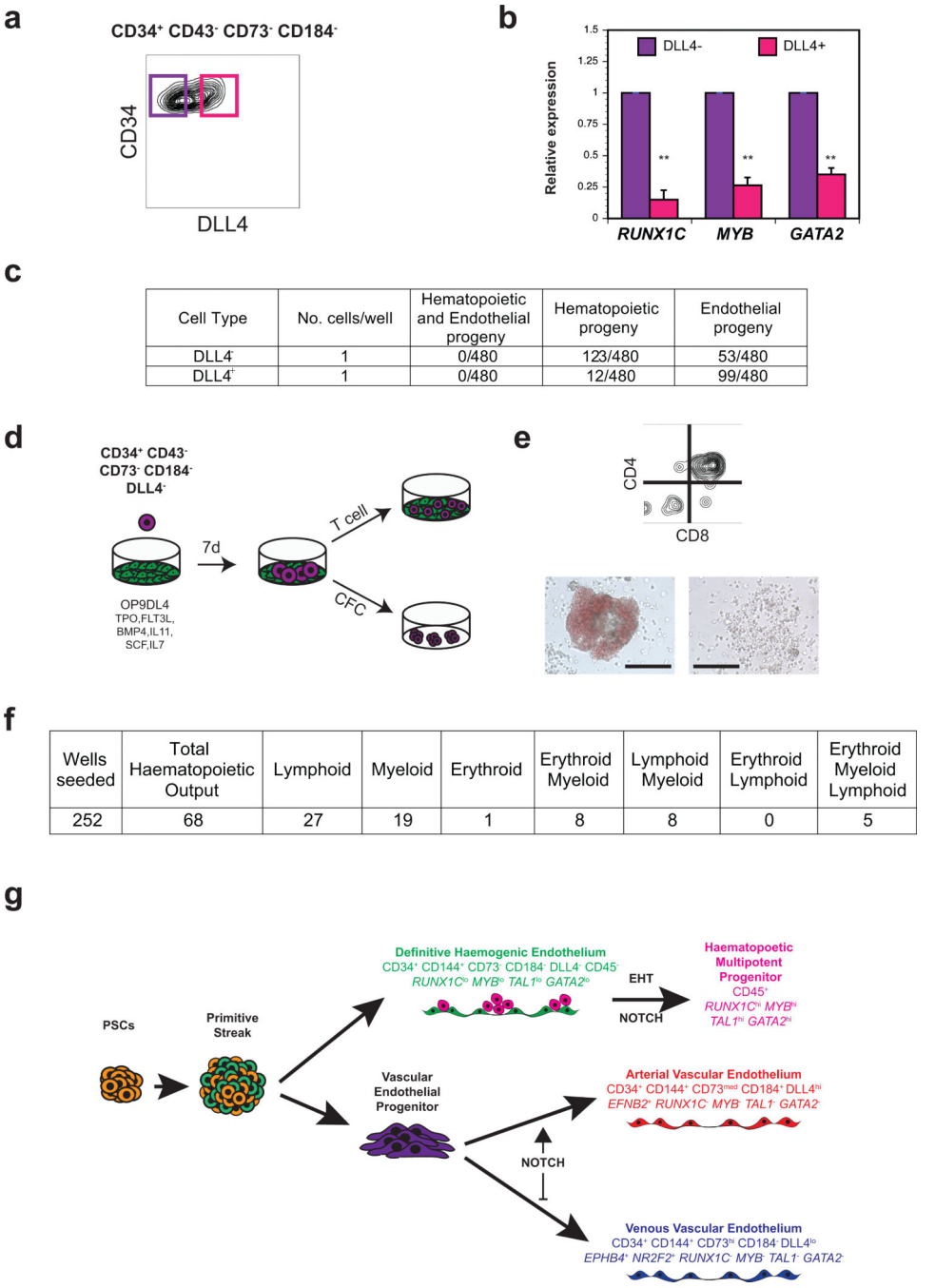

Cell Type	No. cells/well	Hematopoietic and Endothelial progeny	Hematopoietic progeny	Endothelial progeny
DLL4-	1	0/480	123/480	53/480
DLL4+	1	0/480	12/480	99/480

Wells seeded	Total Haematopoietic Output	Lymphoid	Myeloid	Erythroid	Erythroid Myeloid	Lymphoid Myeloid	Erythroid Lymphoid	Erythroid Myeloid Lymphoid
252	68	27	19	1	8	8	0	5

Figure 7. The CD34^{+}CD43^{-}CD73^{-}CD184^{-}DLL4^{-} HE fraction contains cells with multilineage potential

a, Gating strategy used for the isolation of the DLL4 fractions from the day 8 CD34^{+}CD43^{-}CD73^{-}CD184^{-} population. **b,** qRT-PCR analysis of *RUNX1C*, *MYB* and *GATA2* expression in the day 8 CD34^{+}CD43^{-}CD73^{-}CD184^{-}DLL4^{-} (DLL4^{-}) and CD34^{+}CD43^{-}CD73^{-}CD184^{-}DLL4^{+} (DLL4^{+}) fractions. $n = 3$, independent experiments. (Mean ± SEM). ** Student's *t*-test *MYB* and *GATA2* $p = 0.0001$, *RUNX1C* $p < 0.0001$. **c,** Table showing the clonal analysis of the day 8 CD34^{+}CD73^{-}CD184^{-}DLL4^{-} EB population.

Numbers indicate the positive wells containing haematopoietic and/or endothelial cells relative to the total number of wells seeded. Data are compiled from 5 independent experiments. **d,** Scheme depicting the strategy used for identifying multipotent progenitors from the day 8 $CD34^+CD43^-CD73^-CD184^-DLL4^-$ HE. Single $CD34^+CD43^-CD73^-CD184$-$DLL4^-$ HE cells were FACS directly onto OP9-DLL4 stromal cells in microtiter wells and cultured for 7 days to initiate EHT and expansion of the derivative haematopoietic progeny. At this stage, each well was harvested and half the cells were replated onto OP9-DLL4 stroma to assay for T cell potential, while the remaining half were plated in methylcellulose to assay for myeloid and erythroid progenitors. **e,** Flow cytometric analyses showing T lymphocytes and photomicrographs showing erythroid and myeloid colonies generated from a single $CD34^+CD43^-CD73^-CD184^-DLL4^-$ HE progenitor. Scale bars: 100 μm. **f,** Table showing the multilineage clonal analysis of the day 8 $CD34^+CD73^-CD184^-DLL4^-$ EB population. Numbers indicate the positive wells containing T lymphoid, myeloid and/or erythroid cells out of 252 wells seeded. Data in **e** and **f** are compiled from 3 independent experiments. **g,** Model depicting the lineage relationship of HE and VE in hPSC-derived populations. Following primitive-streak/ mesoderm induction, the definitive HE lineage is specified and emerges as a $CD34^+CD43^-$ $CD184^-CD73^-DLL4^-$ $CD45^-$ population by day 8 of differentiation. Under appropriate conditions, the HE undergoes EHT in a NOTCH-dependent manner, giving rise to $CD34^+CD144^+CD45^+$*RUNX1C*$^+$ definitive haematopoietic multipotent progenitors. Alternatively, mesoderm can be specified towards a vascular endothelial fate, generating a progenitor population that can directed to an arterial ($CD73^{med}CD184^+$) or venous fate ($CD73^{hi}$ $CD184^-$) by activation or inhibition of Notch signalling respectively. These endothelial cells derived from the vascular endothelial progenitors are devoid of any haematopoietic activity.